Published in AJSE, Vol:23, Issue: 2
Received on 28th April 2023
Revised on 2nd April 2024
Published on 30th August 2024

AIUB JOURNAL OF SCIENCE AND ENGINEERING
ISSN: 1608 – 3679 (print) 2520 – 4890 (Online)

Design and Performance Analysis of Robust Adaptive Neuro-Fuzzy Inference System-Based Modified P&O Algorithm of MPPT Controller for a Solar PV System

Arnob Chandra Dafader, Md. Rifat Hazari, Shameem Ahmad and Mohammad Abdul Mannan

***Abstract*- Perturb and observe (P&O) is a well-known maximum power point tracking (MPPT) algorithm that is used in solar photovoltaic (PV) systems to increase its efficiency. However, as the PV system uses solar irradiance and temperature for making electric power, the fast change of these two affects the performance of P&O and the efficiency of the PV system. Thus, the P&O algorithm fails to detect maximum power point (MPP) if temperature and irradiance change quickly. Therefore, this paper presents an adaptive neuro-fuzzy inference system (ANFIS) based P&O algorithm of MPPT controller for a solar PV system to solve the issues mentioned earlier. The utilization of the proposed ANFIS in the P&O algorithm can track the fast changes in solar irradiance and temperature to extract the maximum power from the solar PV panel. Comparative analysis has been done on MATLAB/Simulink software for both the traditional P&O and the proposed ANFIS-based P&O algorithm to show the effectiveness of the proposed MPPT controller.**

Keywords: ***Perturb and observe (P&O), adaptive neuro-fuzzy inference system (ANFIS), maximum power point tracking (MPPT), fuzzy logic controller (FLC), artificial neural network (ANN).***

I. Introduction

Seven nations have chosen to outlaw fossil fuels, particularly coal because it releases CO_2 and causes global warming. Sustainable energy comes from renewable sources. Solar energy is one of the renewable energy sources and can be used using PV panels. PV panels must be installed on the rooftops of 50% of government buildings, 20% of homes, 30% of commercial buildings, and 40% of community services buildings in China. In the USA, a solar farm with four pilot systems that has a 2.3 MW capacity has been erected as of 2021 [1]. The use of large-scale renewable energy sources (RESs) has expanded over the past ten years because of the problem of global warming caused by fossil fuel-based power plants and the rising expense of those plants. The popularity of PV panels is the highest among all RESs as their cost is falling [2].

By examining historical growth statistics, it is possible to predict that the annual market will reach 200 GW by 2025 [3]. By the year 2100, it is predicted that 70% of the world's energy will be produced using solar technology, making it one of the most prominent renewable resources in recent years [4].

Solar energy is abundant on earth, and PV panels are simple to install and require little maintenance. Solar energy is also favorable to the environment. The main factor causing the voltage variation of the PV terminal is the nonlinear influence of solar irradiation. The variation in solar irradiation caused a percentage variation in the rated output capacity of a single PV power plant in Portugal between 45 and 90%, according to research [5]. This system, however, has poor efficiency. To address the efficiency issue, the MPPT controller is an integral part of PV systems nowadays [6-8].

PV systems generate power by utilizing temperature and solar radiation. These two factors have an impact on MPP. Maximum power can alter with changes in temperature and irradiation. Therefore, MPPT algorithms are utilized to maintain the PV system's higher efficiency. MPP is detectable by MPPT. If temperature and irradiance are not changed, MPPT should keep MPP constant; if temperature and irradiance are changed, MPPT should find accurate MPP. This will boost the efficiency of the PV system. PV voltage is maintained at a level known as MPP, which is the maximum possible multiplication of PV voltage and current [6]. A well-known MPPT algorithm is P&O. It is simple to use and requires little money to set up [6]. This method, however, struggles to track precise power latency and encounters a steady-state problem with changes in temperature and irradiance. Numerous authors have offered numerous solutions to this problem.

Characteristics of PV systems are nonlinear. Since fuzzy logic control (FLC) has knowledge-based nonlinear structural properties, it is useful for nonlinear systems. Some literature has only mentioned the FLC as a possible way to improve MPPT [6–13] and frequently employed twenty-five rules in the FLC. The authors of [6–9] used five membership functions (MFs) with twenty-five rules, two inputs, and one output. Few

Arnob Chandra Dafader is a student of M.Sc., Department of EEE, American International University-Bangladesh, Dhaka, Bangladesh. E-mail : arnobdafader@gmail.com

Md. Rifat Hazari is a Senior Assistant Professor and Special Assistant of the Department of EEE, American International University-Bangladesh, Dhaka, Bangladesh. E-mail: rifat@aiub.edu

Shameem Ahmad is an Assistant Professor of the Department of EEE, American International University-Bangladesh, Dhaka, Bangladesh. E-mail: ahmad.shameem@aiub.edu

Mohammad Abdul Mannan is a Professor and Associate Dean of the Faculty of Engineering, American International University-Bangladesh, Dhaka, Bangladesh. Email: mdmannan@aiub.edu

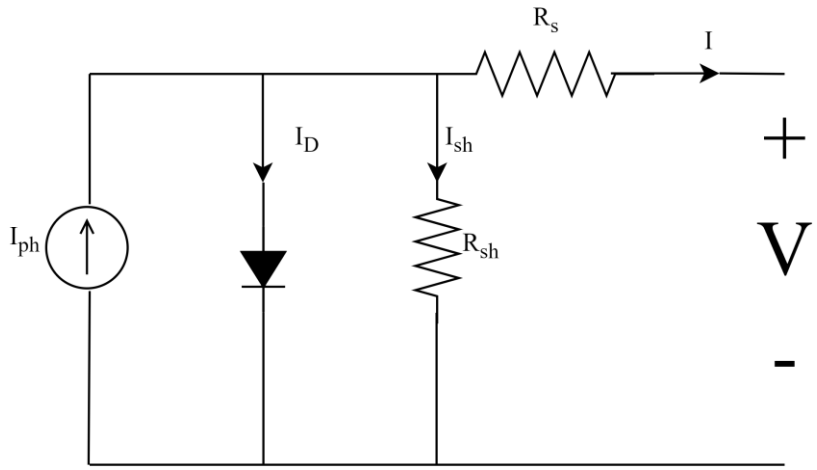

Fig. 1: Single-diode model of PV cell.

authors in a few works of literature use seven MFs with forty-nine rules [10], [11].

Three MFs with nine rules were also used by certain authors [12]. The authors of Ref. [13] used two MFs with two rules and the PV current "*I*" as the input for the FLC to achieve their best result. Despite producing better results, FLC-based MPPT has a major flaw in the architecture of its MFs, and creating rules is a difficult task. The layout of the MFs and rules determines how effective the system is. Artificial neural networks (ANN), on the other hand, are appropriate for nonlinear systems because of their capacity for universal approximation and their adaptable structure, which enables the capture of complicated nonlinear phenomena. Authors [14–18] have used ANN-based MPPT. The way ANNs are trained influences how well they perform. Nodes of ANN must be tuned regularly as they get older. An ANN that has been trained for one capacity of a PV system cannot be used for another capacity. ANFIS combines FLC with neural networks and is also utilized for nonlinear systems [19].

The ANFIS-based P&O method is proposed in this research. The proposed system's contribution gets around P&O's drawbacks. P&O's primary drawback is that it takes a long time to identify MPP when temperature and irradiance change rapidly [6]. The proposed technique is more efficient than traditional P&O and other systems already in use. Its performance is evaluated using actual temperature and irradiance numbers as well as uniform and nonuniform values. Comparisons were made between the suggested method's performance and that of other currently used methods and the traditional P&O algorithm. The suggested ANFIS-based P&O outperformed the others. A detailed presentation of the suggested ANFIS-based P&O design methodology is also made.

In section II the PV model is shown. In section III, DC-DC boost converter is discussed. Traditional P&O is reviewed in section IV. Section V is based on ANFIS. In sections VI and VII, the proposed method and result were discussed, respectively.

II. PV Model

PV models come in single-diode and double-diode varieties. The single-diode model is more accurate and less complex than the double-diode model [20]. Fig. 1 shows the single-diode PV model.

Being a photodiode, the solar cell produces an electron-hole pair when exposed to sunlight, which causes current to flow. KCL was used to discover this in the following equation [7].

$$I=I_{ph}-I_D-I_{sh} \quad (1)$$

$$I = I_{ph} - I_0\left\{\exp\left[\frac{(V-R_SI)}{V_Ta}\right]-1\right\} - \frac{V+R_SI}{R_{\text{sh}}} \quad (2)$$

It is discovered in equations (1) and (2) that output power is influenced by temperature and irradiance.

The PV system's current, $I_{ph,}$ is being discussed here. The reverse saturation current is indicated by I_0. R_s is a series-connected resistor, and R_{sh} is a parallel resistor. The term V_T stands for thermal voltage.

$$V_T = \frac{N_SKT}{q} \quad (3)$$

Here, N_s is the number of series-connected cells, q is the charge of the electrons, T is the temperature in Kelvin, and K stands for the Boltzmann constant. Fig. 2 represents the *I-V* & *P-V* characteristics of the PV system. The *I-V* & *P-V* characteristics for varying irradiance are shown in Fig. 3. It is discovered that MPP is rising as irradiance rises. Short circuit current (I_{sc}), which similarly rises with an increase in irradiance, causes power to rise as well. MPP also rises as a result.

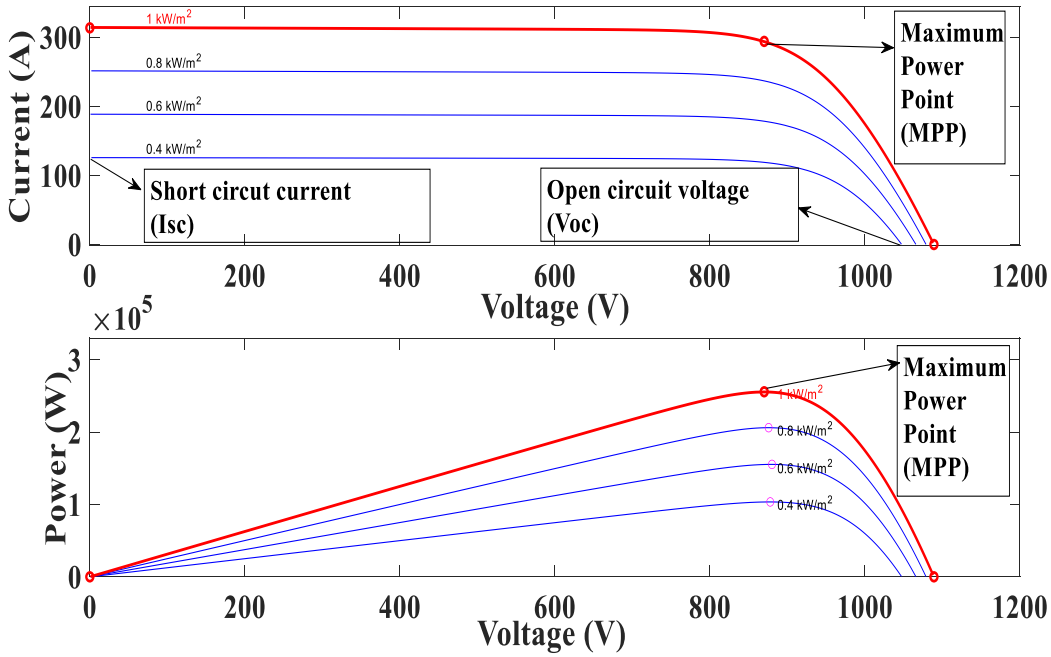

Fig. 2: I-V & P-V characteristics for changing irradiance.

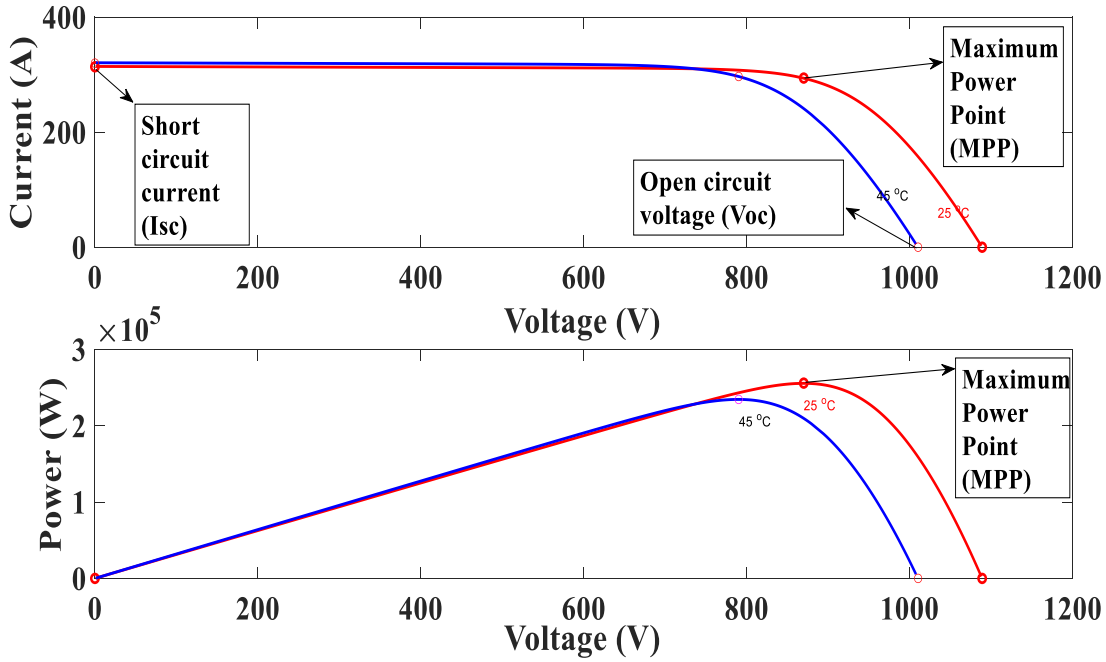

Fig. 3: I-V & PV characteristics for changing temperature.

Fig. 3 shows that whereas open circuit voltage (V_{oc}) changes significantly with temperature, I_{sc} changes just slightly. V_{oc} lowers as the temperature rises. Consequently, the fill factor likewise drops, and efficiency suffers as a result.

III. DC-DC Converter

In the proposed method, the DC-DC boost converter is used to transfer power to the load which is shown in Fig. 4. A duty cycle signal ($0<D<1$) is generated by pulse width modulation (PWM) and the generated signal controls the IGBT.

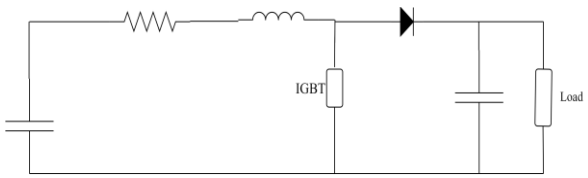

Fig. 4: DC-DC boost converter.

The input and output variables relationship are given below [10]:

$$V_o = V_{in}/(1-D) \quad (4)$$

$$I_{\text{out}} = (1-D)I_{\text{in}} \quad (5)$$

Equivalent resistance (R_{eq}) is represented in equation 6.

$$R_{eq} = R_{in}\,(1-D)^2 \quad (6)$$

The duty cycle can be obtained according to the maximum power transfer theorem as below:

$$R_{in} = V_{in}/I_{in} = R_o(1-D)^2 \Longrightarrow D = 1 - \sqrt{\frac{R_{in}}{R_o}} \quad (7)$$

When R_{eq} is equal to output resistance (R_o) the maximum power transfer happens.

$$L = \frac{(V_o - V_{in})V_{in}}{f(\triangle I)V_o} \quad (8)$$

$$C = \frac{(V_o - V_{\text{in}})I_{\text{out}}}{f(\Delta V)V_o} \quad (9)$$

Equations 8 and 9 illustrate the functions of the inductor (L) and capacitor (C).

IV. Traditional Perturb and Observe (P&O) Algorithm

The algorithm P&O is used to find MPP. The P&O algorithm is displayed in Fig. 5 and in Fig. 6 tracking of MPP is shown.

This algorithm begins by obtaining the PV system's voltage and current values. It then observes the power shift. The duty cycle remains unchanged if the change in power, $DP = 0$, remains constant. But if not, it then determines whether $DP>0$. By varying the duty cycle, it can raise or lower the value of DV depending on the value of DP.

The duty cycle is indicated as "D" in Fig. 5. The duty cycle is increased or decreased by adding or removing a fixed step size, *deltaD*. Here, *deltaD* is a fixed amount. The drawback of P&O is that oscillation will occur around MPP if the step size is big. The identification of MPP will take longer, however, if the step size is fixed [6].

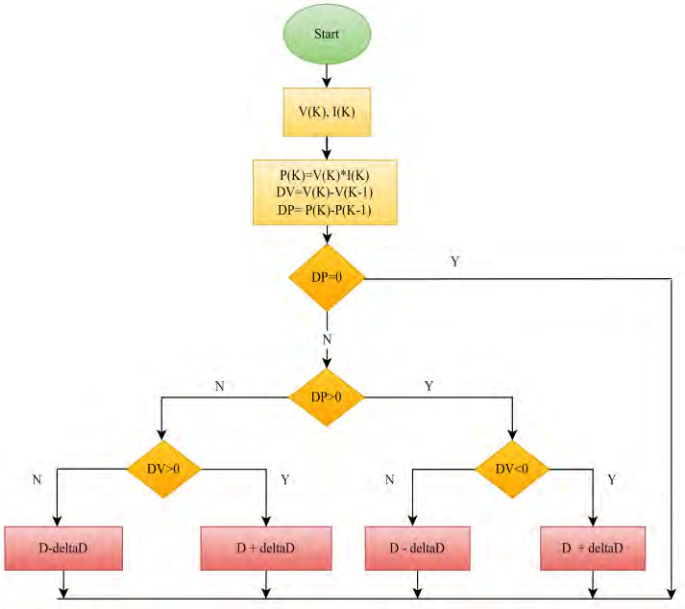

Fig. 5: Perturb and observe (P&O) algorithm.

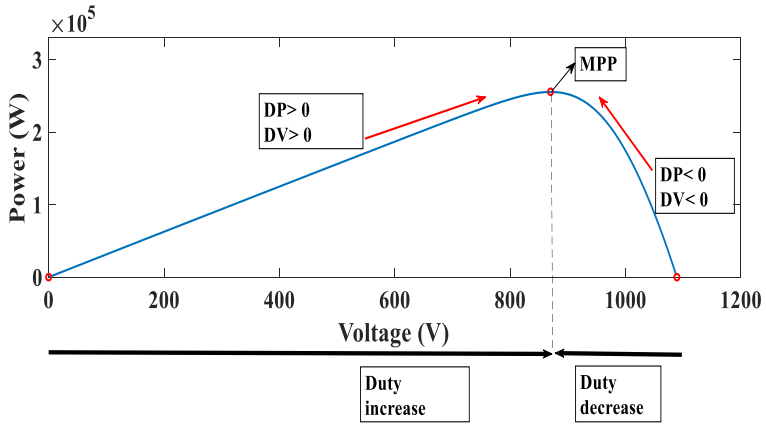

Fig. 6: Tracking of MPP.

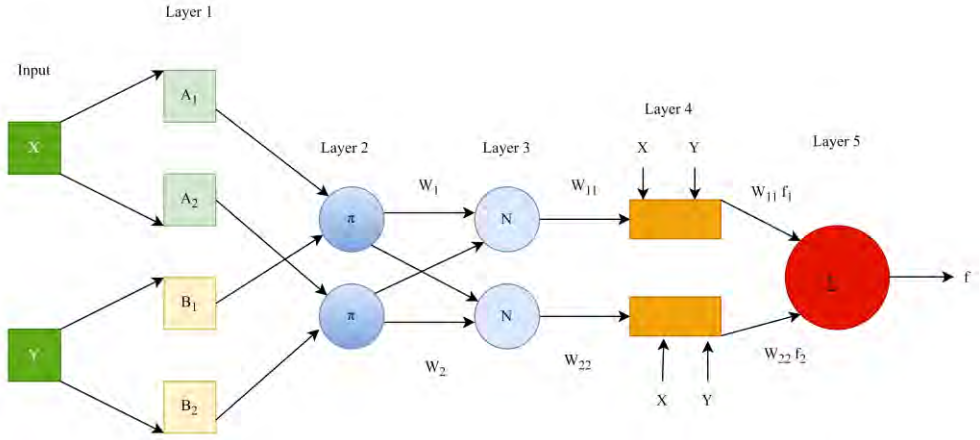

Fig. 7: ANFIS structure.

V. Adaptive Neuro-Fuzzy Inference System (ANFIS)

In 1993 Jang developed ANFIS. Its method for learning data is straightforward. This method is simple to use and doesn't require the assistance of a professional human. Additionally, it learns quickly and with great accuracy. ANFIS solves issues by fusing language and numerical techniques. It describes a complex sort of system and applies fuzzy IF-THEN logic. ANFIS makes use of fuzzy logic (FL) and a neural network to translate provided input into the desired output. Thus, it is an FL and neural network combo [19]. In general, ANFIS has the same components as FL and neural networks. Fuzzification, knowledge bases, neural networks, and defuzzification are the components of these layers. Layer 1 accepts input values or MFs. The weights of each MF are checked in Layer 2, which is referred to as the MFs layer. It receives input from Layer 1 and outputs all inputs as fuzzy sets. The ruling layer is referred to as layer 3. The nodes of neurons make up this layer. In this layer, each rule's activation level is compared, and each node in this layer matches fuzzy rules' preconditions. The defuzzification layer is located at Layer 4. This layer provides the output values that result from the inference of rules. The output layer is layer 5. It resolves a fuzzy classification into a clear value [21]. The rules are presented below:

Rule 1: IF X is A1 and Y is B1, then F1 = P1X+ Q1Y + r1

Rule 2: IF X is A2 and Y is B2, then F2 = P2X+ Q2Y + r2

Fig. 7 represents the ANFIS structure. Fixed nodes are represented by circular blocks, while adaptive nodes are represented by square blocks. In this case, *X* and *Y* stand for input. *Ai* and *Bi* are the representations of fuzzy sets. Here, *Pi*, *Qi*, and *ri* are used to display the design parameter.

Fig. 7 depicts Layer 1 as being represented by square blocks. It is an adaptable node, then. Layer 1's output is the FL membership function. The output of Layer 1 is shown in the following equation.

$$\theta_i^1 = \mu_{Ai}(\mathrm{X}) \tag{10}$$

$$\theta_i^1 = \mu_{\mathrm{Bi}}(\mathrm{Y}) \tag{11}$$

Here *Ai* and *Bi* are linguistic variables of input *X* and *Y*. μ_{Ai} and μ_{Bi} can take any type of FL membership function.

$$\mu_{Ai}(x) = \exp\left\{-\left(\frac{x-c_i}{a_i}\right)^2\right\} \tag{12}$$

Layer 2 is represented by circular blocks in Fig. 7 and is a fixed node. It is indicated by π. This layer fuzzifies input using the fuzzy AND operator. The following equation illustrates how it works.

$$\theta_i^2 = \mathrm{W}_i = \mu_{Ai}(\mathrm{X}) \times \mu_{Bi}(\mathrm{Y}), i = 1{,}2 \tag{13}$$

Here, W_i denotes the output of Layer 2.

Layer 3 also includes fixed nodes. *N* indicates that it. These nodes play a part in normalizing the firing strengths that are obtained from the preceding layer.

$$\theta_i^3 = W_{ii} = \frac{w_i}{W_1+W_2} \tag{14}$$

Here, W_{ii} is the output of Layer 3.

Fig. 7 shows that Layer 4 is denoted by a square layer and that it is an adaptive layer. Its primary function is to do the product of first-order polynomials with normalized firing strengths.

$$\theta_i^4 = \mathrm{W}_{ii}\mathrm{F}_i = \mathrm{W}_{ii}(P_iX + Q_iY + \mathrm{r}_i) \tag{15}$$

In Layer 5, there is one node only and it is a fixed node. It is denoted by $\sum$. The task of this node is to make a summation of all input signals. The equation of Layer 5 is given below.

$$\theta_i^5 = \text{overall} - \text{output} = \sum_i W_{ii}F_i = \frac{\sum_i W_iF_i}{\sum_i W_i} \tag{16}$$

VI. Proposed ANFIS-based Modified P&O Algorithm

The ANFIS-based P&O model suggested in the article is shown in Fig. 8. The ANFIS will use temperature

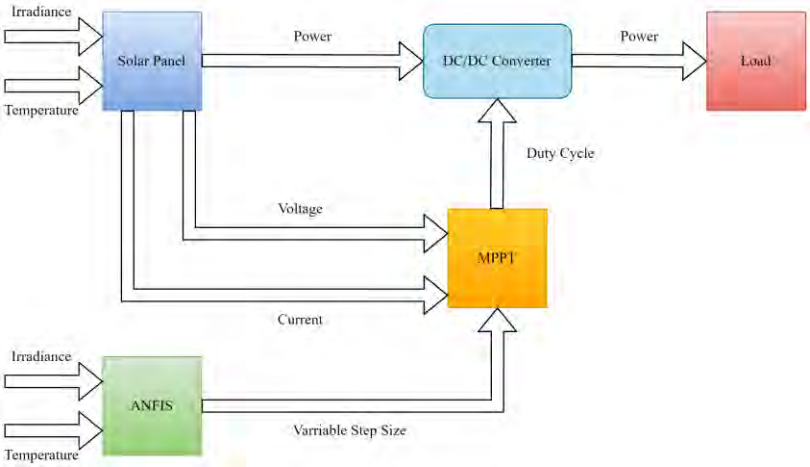

Fig. 8: Block diagram of the proposed method.

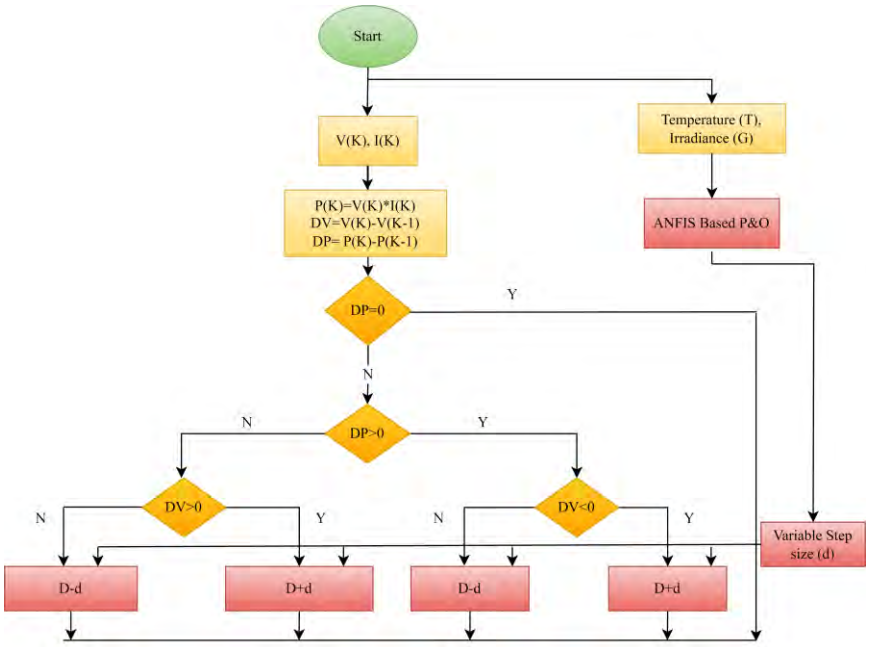

Fig. 9: Proposed ANFIS-based P&O algorithm flowchart.

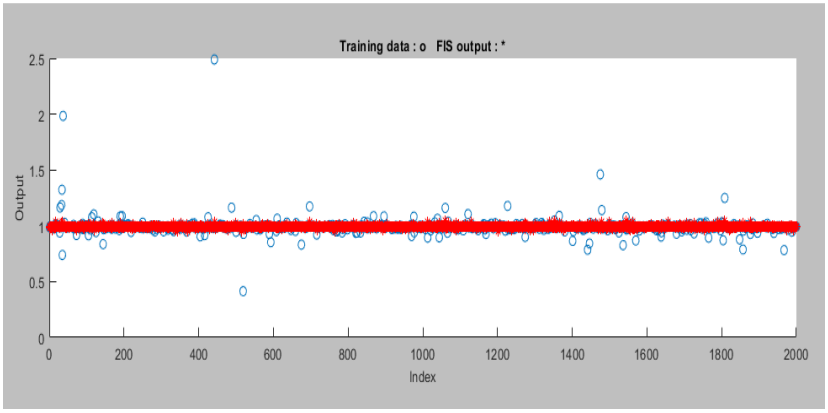

Fig. 10: Training output of ANFIS.

and irradiance as inputs and provide a changeable step size *d* as an output. This output will be sent to P&O and it provides an efficient duty cycle that provides a useful switching frequency for the DC-DC converter.

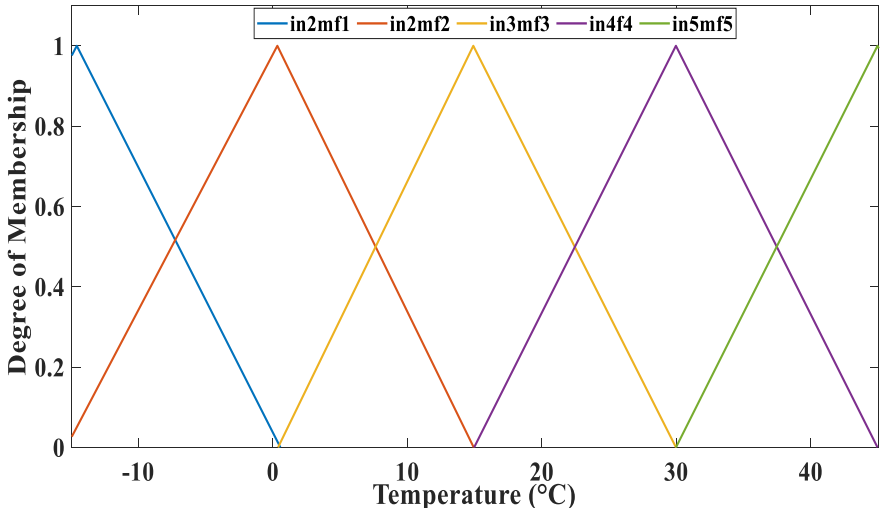

Fig. 11: Membership function for temperature.

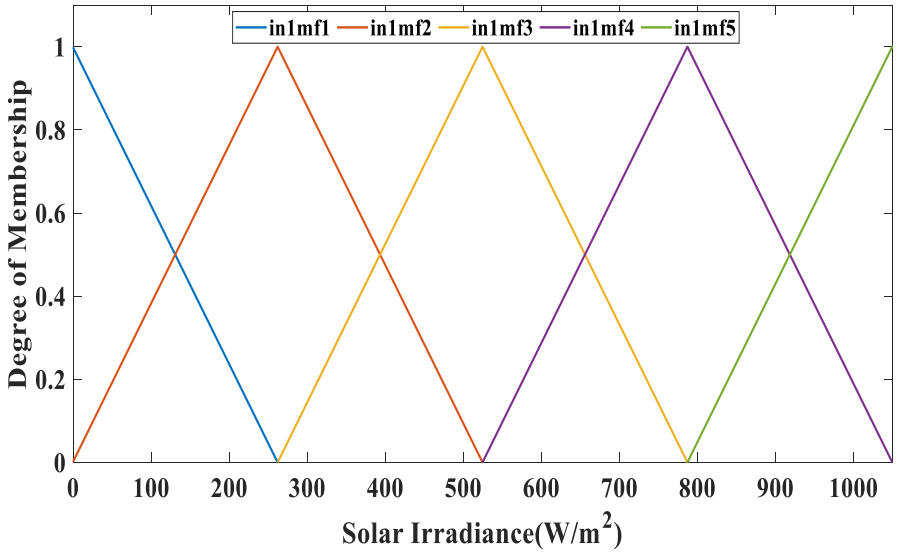

Fig. 12: Membership function for irradiance.

A hybrid approach using nonlinear and linear Layer 2 and Layer 4 parameters is employed for updating. The hybrid ANFIS algorithm combines the Least-square approach and the steepest descent method. The hybrid algorithm exhibits both forward propagation and back-propagation kinds of propagation. During forward propagation, the output of the node is forwarded up to Layer 4, and liner parameters are changed using the least-squares method. The gradient descent method adjusts the linear parameters while the erroneous signal propagates backward. The efficient decrease of search space dimensions during training gives the hybrid algorithm a faster rate of convergence than traditional back-propagation methods. The datasets were constructed by simulating the solar PV array under various situations by varying irradiance and temperature values, and ANFIS was trained using these datasets [22][23].

Short circuit current, maximum current at MPP, open circuit voltage, maximum voltage at MPP, temperature and voltage coefficients, standard irradiance, and standard temperature have all been initialized in the code for training the ANFIS. The code has received the temperature and irradiance data for training. Variable step sizes have been created in the code using these solar panel-related metrics as well as temperature and irradiance data. After training of ANFIS, the block is implemented in the main model in Simulink.

The flowchart of the proposed approach is shown in Fig. 9. ANFIS is initially trained using various temperature and irradiance parameters. The ANFIS, which plots MFs and generates appropriate rules, has been trained using 2000 data. It was demonstrated in Section 4 that the P&O algorithm determines the duty cycle based on the PV voltage and current readings. This algorithm's fixed step size for changing the duty cycle has some downsides, including a longer detection time for MPP and oscillation near MPP. By measuring temperature and irradiance, ANFIS will generate variable step size *d* in the described approach. The P&O

algorithm will then receive it. The duty cycle is then modified in the P&O method by adding or subtracting by the configurable step size *d*. Fig. 6 illustrates how *DV* changed along with the duty cycle change. The shortcomings of conventional P&O have been successfully solved since variable step size has been used, as in the suggested method.

Fig. 10 shows the training output of ANFIS. For training ANFIS at the very beginning temperature and irradiance data were collected. In the collected data, the chosen temperature range was -15 °C to 45 °C, and the irradiance range was 0 W/m^2 to 1050 W/m^2. The developed ANFIS can operate effectively under a variety of operating situations because of these parameters' wide and dynamic range for temperature and irradiation and can produce effective variable step size *d* for the operation of P&O perfectly. 100 epoch is used here. The root means square error (RMSE) of ANFIS 0.048992. After completing training, ANFIS produces MFs and Sugeno fuzzy model. The main task of this rule is creating perfect variable step size *d*. Five MFs is used for temperature and irradiance and for this reason RMSE is low.

Fig. 11 and Fig. 12 represent MFs for temperature and irradiance respectively. Here, the range of temperature is -15 °C to 45 °C. and the range of irradiance is 0 W/m^2 to 1050 W/m^2. Triangle MFs are used for both irradiance and temperature. 25 rules are used in this model.

A fixed step size is used to adjust the duty cycle in the classic P&O technique, which has issues with oscillation around MPP and current MPP detection. The ANFIS will produce varied step sizes for the suggested approach to solve these problems as a function of temperature and irradiance changes. The Boost Converter will use the new duty cycle produced by the P&O MPPT algorithm to generate a new switching frequency.

VII. Simulation Results and Analysis

The work has been simulated in MATLAB/Simulink software. This work makes use of the Soltech 1STH-215-P module. There are 40 parallel strings and 30 modules per string that are connected in series. A DC-DC converter has been employed with the boost converter. Figs. 13 and 14 show the real value of solar irradiance and temperature, respectively.

The output voltage for a real value for temperature and irradiance is shown in Fig. 15. Traditional P&O alters the duty cycle with a set step size, as described in section 4. As a result, if the step size is small, MPP will take a long time to detect and will oscillate. On the other side, if the step size is large, MPP will be detected more quickly, but oscillation around MPP will become an issue. In Fig. 15, because the step size was large, it detected a higher voltage value than the suggested way. The excessive step size caused the duty cycle to change more frequently than was necessary. The output current for real values of temperature and irradiance is shown in Fig. 16. The figure makes it obvious that irradiance has an impact on how the PV current changes. I_{sc} changes significantly with changes in irradiance, as demonstrated in Fig. 2.

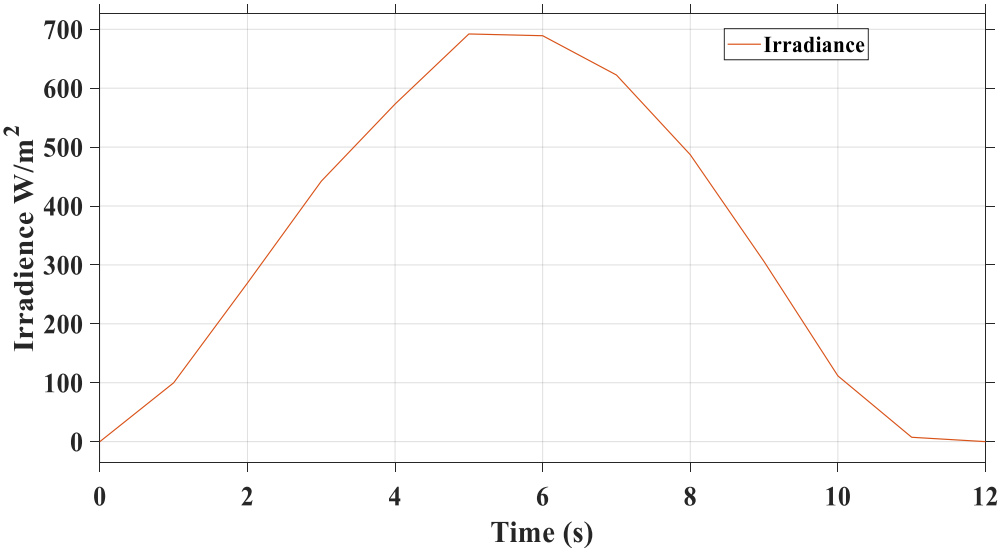

Fig. 13: Real value of irradiance for January.

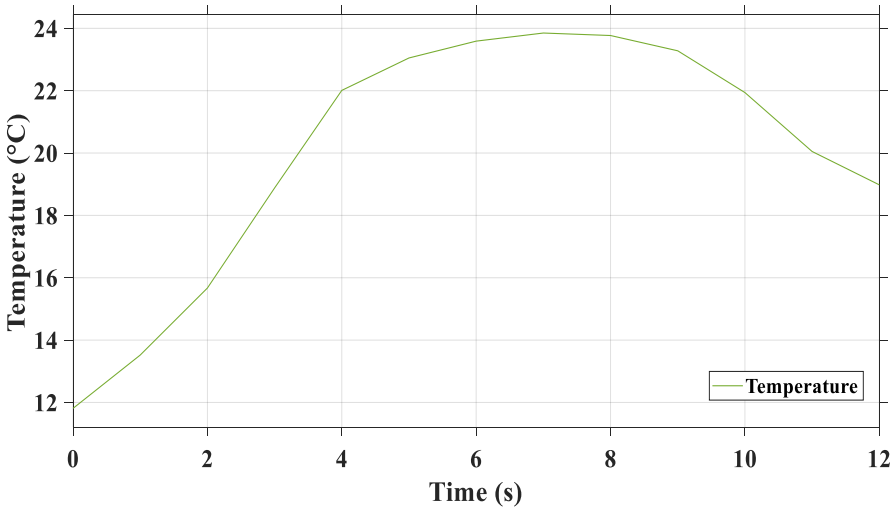

Fig. 14: Real value of temperature for January.

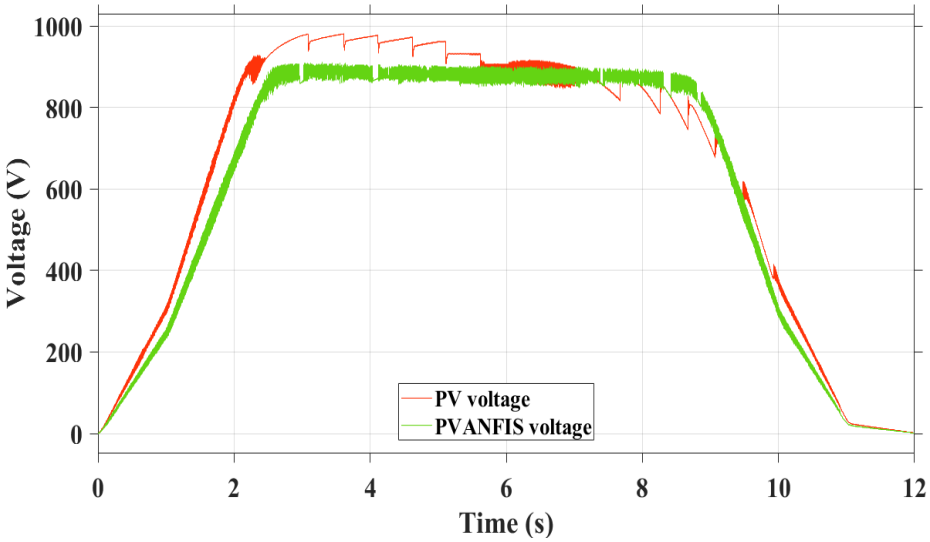

Fig. 15: Output voltage for real value of temperature and irradiance.

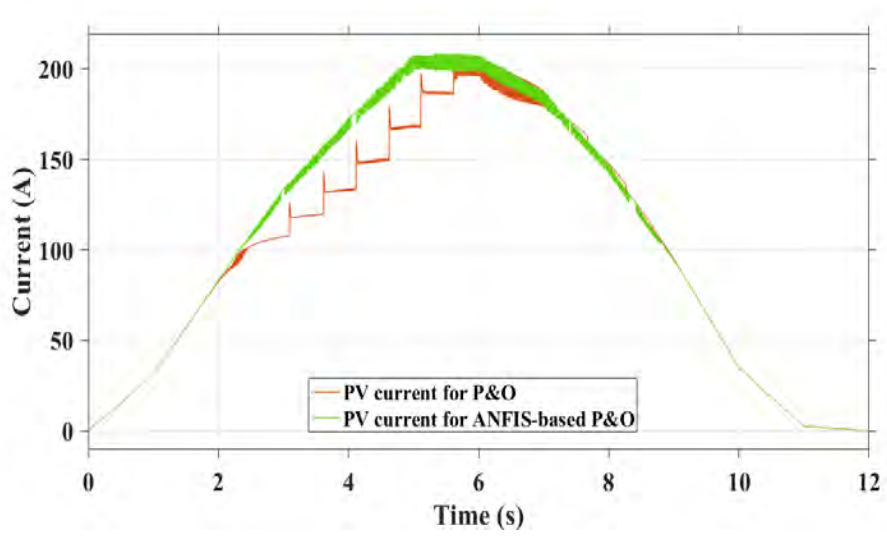

Fig. 16: Output current for real value of temperature and irradiance.

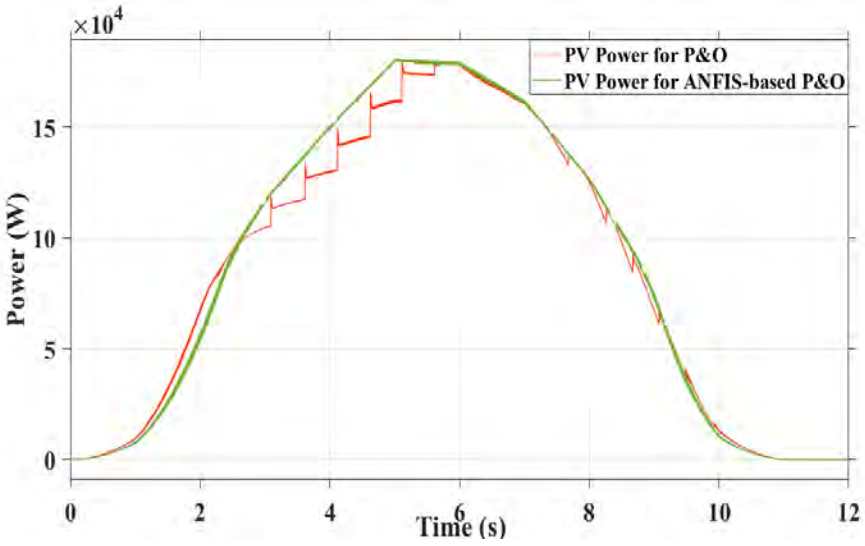

Fig. 17: Output power for real value of temperature and irradiance.

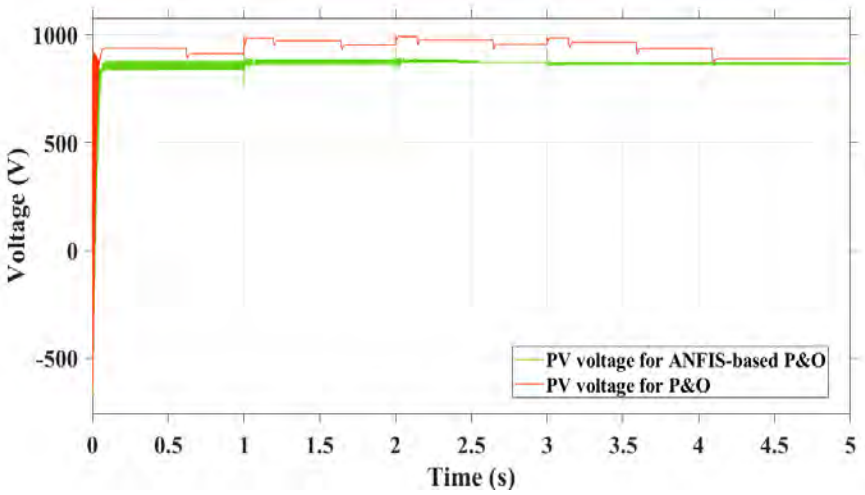

Fig. 18: Output voltage of ANFIS-based P&O and P&O for constant temperature and varying irradiance.

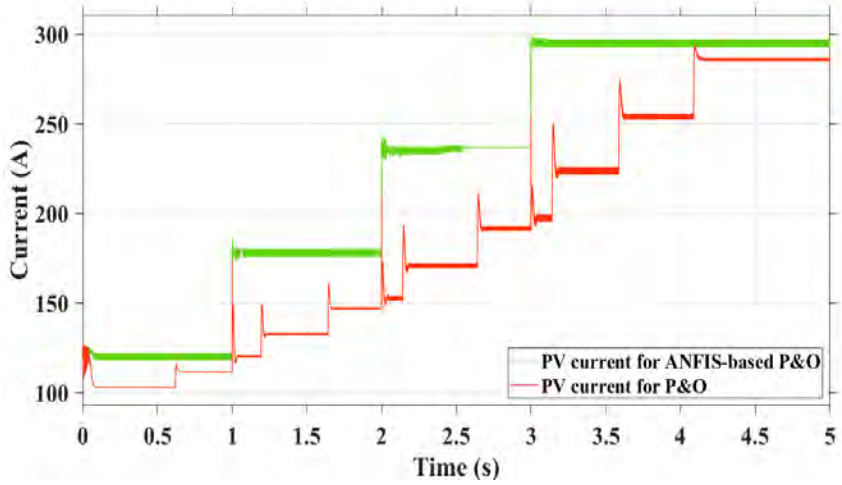

Fig. 19: Output current of ANFIS-based P&O and P&O for constant temperature and varying irradiance.

The output power for real values of temperature and irradiance is shown in Fig. 17. According to Fig. 15, the excessive step size caused P&O to modify the duty cycle more than was necessary and utilize more

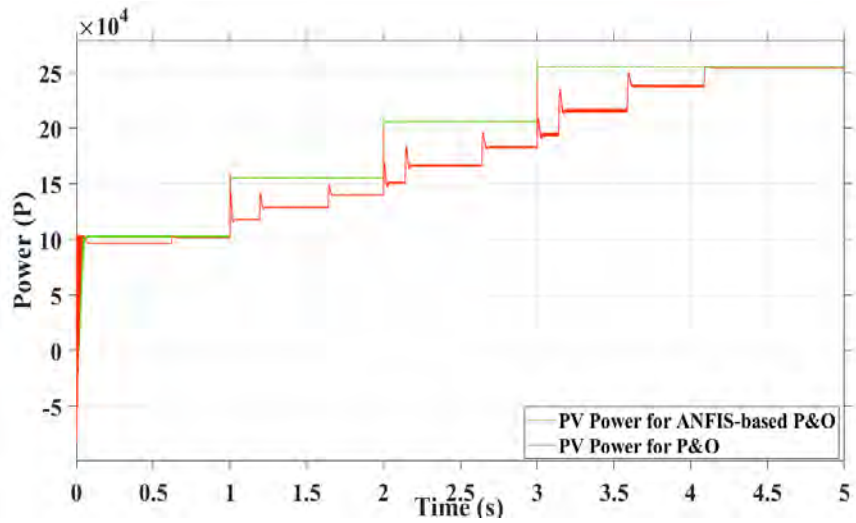

Fig. 20. Output power of ANFIS-based P&O and P&O for constant temperature and varying irradiance.

voltage than was required. As a result, classic P&O took longer to detect MPP when input irradiance and temperature changed rapidly because oscillation occurred near MPP during that time. Conventional P&O was unable to identify MPP in time as a result, and power loss resulted. The proposed ANFIS-based P&O method, on the other hand, offered changeable step size to P&O with the change in temperature and irradiance. So, the suggested method has identified MPP successfully. As a result, the power loss is less than conventional P&O.

Fig. 18 shows the output voltage and Fig. 19 shows the output current of ANFIS-based P&O and P&O for constant temperature and varying irradiance. As mentioned earlier in Fig. 15, in Fig. 18, because of the large step size P&O is detecting a larger voltage value than the suggested method.

Fig. 20 shows the output power of ANFIS-based P&O and P&O for constant temperature and varying irradiance. It shows that ANFIS-based P&O can detect MPP faster than traditional P&O. As previously stated, P&O has poor accuracy for detecting rapid changes in temperature and irradiance. Additionally, it takes a long time to identify MPP due to the set step size. However, the proposed method uses variable step sizes, which allows it to detect MPP more quickly than the conventional P&O algorithm. Moreover, the proposed system is more efficient than traditional P&O. Here, the temperature is maintained at 25°C while the irradiance is varied between 400, 600, 800, and 1000 W/m^2. It took 0.7 s for conventional P&O to detect MPP at 400 W/m^2. On the other hand, ANFIS-based P&O accurately and immediately detected the MPP. The irradiance changed to 600 W/m^2 at 1 s, and the suggested approach simultaneously recognized MPP with 100% accuracy while standard P&O was unable to do so. Irradiance adjusted to 800 W/m^2 in 2 s. Additionally, in this instance, traditional P&O failed to detect MPP at 2 s, but the suggested technique did it with 100% accuracy. Irradiance increases to 1000 W/m^2 in 3 s. In this instance, traditional P&O recognized MPP in 4.1 s while ANFIS-based P&O did so at 3 s with an accuracy of 99.92%. As a result, it has been determined that ANFIS-based P&O has performed better than traditional P&O.

Table 1. Efficiency of ANFIS-based P&O.

Irradiance (W/m^2)	Temp. (°C)	Ref. Power (W)	Output Power (W)	Efficiency
400	25	103500	103500	100%
600	25	155400	155400	100%
800	25	206100	206100	100%
1000	25	255800	255600	99.92%
			Average	99.98%

Table 1 shows that the efficiency of ANFIS-based P&O is 99.98% and the error is 0.02.

Table 2. Comparison of ANFIS-based P&O and other algorithms.

Method	**Efficiency**
ANFIS-based P&O [Proposed Model]	99.98%
FIS [13]	99.12%
ANN [14]	Up to 99.68%
ANN [18]	Above 90%

Table 2 shows that the ANFIS-based P&O is showing better results than other existing methods. As it is using variable step sizes for detecting MPP with the change of temperature and irradiance so that it can track it faster and accurately with better efficiency.

VIII. Conclusions

This paper suggests a robust method for getting around the P&O algorithm's constraints. The old P&O MPPT algorithm's fundamental drawback was its set step size, which makes it difficult to detect MPP. The proposed

approach has, however, circumvented the issue by generating variable step sizes. The effectiveness of the suggested strategy has been evaluated under a variety of circumstances and using actual temperature and irradiance data. With an efficiency of 99.98%, this ANFIS-based P&O MPPT algorithm has demonstrated superior performance than existing MPPT algorithms. Thus, this suggested system has minimal power loss. The future plan of this work is to connect the genetic algorithm (GA) with this ANFIS-based P&O.

References

[1] "RENEWABLES 2022 GLOBAL STATUS REPORT." https://www.ren21.net/gsr-2022/ (accessed Apr. 05, 2023).

[2] M. R. Hazari, E. Jahan, M. A. Mannan, and N. Das, "Transient stability enhancement of a grid-connected large-scale pv system using fuzzy logic controller," *Electronics (Switzerland)*, vol. 10, no. 19, Oct. 2021, doi: 10.3390/electronics10192437.

[3] A. Ahmed, M. R. Hazari, E. Jahan, and M. A. Mannan, "A Robust Control Strategy to Improve Low Voltage Ride-through of a Grid-connected Photovoltaic System," *International Journal of Power and Energy Systems*, vol. 41, no. 1, 2021, doi: 10.2316/j.2021.203-0299.

[4] S. M. I. Rahman*, M. R. Hazari, S. U. Hani, B. B. Pathik, M. A. Mannan, A. Mahfuz, M. K. Alam, M. K. Hassan.*, "Primary frequency control of large-scale pv-connected multi-machine power system using battery energy storage system," *International Journal of Power Electronics and Drive Systems*, vol. 12, no. 3, pp. 1862–1871, Sep. 2021, doi: 10.11591/ijpeds.v12.i3.pp1862-1871.

[5] M. Sakiluzzaman, M. S. Hasan, K. Anam, M. Almustanjid Akash, and M. R. Hazari, "Voltage Stability Augmentation of Hybrid Power System using Robust Reactive Power Control Strategy of PV Plant," International Journal of Renewable Energy Research, vol. 11, no. 3, September, 2021, doi:10.20508/ijrer.v11i3.12245.g8289.

[6] J. Macaulay and Z. Zhou, "A fuzzy logical-based variable step size P&O MPPT algorithm for photovoltaic system," *Energies (Basel)*, vol. 11, no. 6, Jun. 2018, doi: 10.3390/en11061340.

[7] H. S. Lee and J. J. Yun, "Advanced MPPT algorithm for distributed photovoltaic systems," *Energies (Basel)*, vol. 12, no. 18, Sep. 2019, doi: 10.3390/en12183576.

[8] D. Remoaldo and I. S. Jesus, "Analysis of a traditional and a fuzzy logic enhanced perturb and observe algorithm for the mppt of a photovoltaic system," *Algorithms*, vol. 14, no. 1, Jan. 2021, doi: 10.3390/a14010024.

[9] M. N. Ali, K. Mahmoud, M. Lehtonen, and M. M. F. Darwish, "An Efficient Fuzzy-Logic Based Variable-Step Incremental Conductance MPPT Method for Grid-Connected PV Systems," *IEEE Access*, vol. 9, pp. 26420–26430, 2021, doi: 10.1109/ACCESS.2021.3058052.

[10] N. Priyadarshi, F. Azam, A. K. Bhoi, and S. Alam, "An Artificial Fuzzy Logic Intelligent Controller Based MPPT for PV Grid Utility," in *Lecture Notes in Networks and Systems*, Springer, 2019, pp. 901–909. doi: 10.1007/978-981-13-1217-5_88.

[11] S. M. Sadek, F. H. Fahmy, A. E.-S. A. Nafeh, and M. A. El-Magd, "Fuzzy P & O Maximum Power Point Tracking Algorithm for a Stand-Alone Photovoltaic System Feeding Hybrid Loads," *Smart Grid and Renewable Energy*, vol. 05, no. 02, pp. 19–30, 2014, doi: 10.4236/sgre.2014.52003.

[12] A. Aurairat and B. Plangklang, "An Alternative Perturbation and Observation Modifier Maximum Power Point Tracking of PV Systems," *Symmetry (Basel)*, vol. 14, no. 1, Jan. 2022, doi: 10.3390/sym14010044.

[13] L. Farah, A. Hussain, A. Kerrouche, C. Ieracitano, J. Ahmad, and M. Mahmud, "A highly-efficient fuzzy-based controller with high reduction inputs and membership functions for a grid-connected photovoltaic system," *IEEE Access*, vol. 8, pp. 163225–163237, 2020, doi: 10.1109/ACCESS.2020.3016981.

[14] S. D. Al-Majidi, M. F. Abbod, and H. S. Al-Raweshidy, "A particle swarm optimisation-trained feedforward neural network for predicting the maximum power point of a photovoltaic array," *Eng Appl Artif Intell*, vol. 92, Jun. 2020, doi: 10.1016/j.engappai.2020.103688.

[15] I. Haseeb *et al.*, "Solar power system assessments using ann and hybrid boost converter based mppt algorithm," *Applied Sciences (Switzerland)*, vol. 11, no. 23, Dec. 2021, doi: 10.3390/app112311332.

[16] L. Chen and X. Wang, "Enhanced MPPT method based on ANN-assisted sequential Monte–Carlo and quickest change detection," *IET Smart Grid*, vol. 2, no. 4, pp. 635–644, Dec. 2019, doi: 10.1049/iet-stg.2019.0012.

[17] L. Bouselham, M. Hajji, B. Hajji, and H. Bouali, "A New MPPT-based ANN for Photovoltaic System under Partial Shading Conditions," in *Energy Procedia*, Elsevier Ltd, Mar. 2017, pp. 924–933. doi: 10.1016/j.egypro.2017.03.255.

[18] J. M. Lopez-Guede, J. Ramos-Hernanz, N. Altın, S. Ozdemir, E. Kurt, and G. Azkune, "Neural Modeling of Fuzzy Controllers for Maximum Power Point Tracking in Photovoltaic Energy Systems," *J Electron Mater*, vol. 47, no. 8, pp. 4519–4532, Aug. 2018, doi: 10.1007/s11664-018-6407-2.

[19] A. Al-Hmouz, J. Shen, R. Al-Hmouz, and J. Yan, "Modeling and simulation of an Adaptive Neuro-Fuzzy Inference System (ANFIS) for mobile learning," *IEEE Transactions on Learning Technologies*, vol. 5, no. 3, pp. 226–237, 2012, doi: 10.1109/TLT.2011.36.

[20] M. K. Islam, M. A. Mannan and M. R. Hazari, "Fault Ride-Through and Transient Stability Augmentation of Grid-Connected PV Station Using Virtual Synchronous Generator" AIUB Journal of Science and Engineering (AJSE), Vol. 20, No. 4, pp. 118-126, Dec. 2021.

[21] K. Premkumar and B. V. Manikandan, "Adaptive Neuro-Fuzzy Inference System based speed controller for brushless DC motor," *Neurocomputing*, vol. 138, pp. 260–270, Aug. 2014, doi: 10.1016/j.neucom.2014.01.038.
[22] M. K. J. Rathi and Ali, "NFC Design using ANFIS for Power Electronics Circuits," International Journal of Innovative Research in Electrical, Electronics, Instrumentation and Control Engineering, vol. 4, pp. 2321–5526, 2016, doi: 10.17148/IJIREEICE.2016.4303.
[23] K. Premkumar and B. V. Manikandan, "Stability and Performance Analysis of ANFIS Tuned PID Based Speed Controller for Brushless DC Motor," *Curr Signal Transduct Ther*, vol. 13, no. 1, pp. 19–30, Feb. 2018, doi: 10.2174/1574362413666180226105809.

Arnob Chandra Dafader was born in Khulna, Bangladesh, in 1998. He received his B.Sc. Engg. Degree in Electrical and Electronic Engineering from American International University-Bangladesh (AIUB) in January 2021 and MSc is going on in Electrical and Electronic Engineering from AIUB. In 2023 he joined ServiceEngine Ltd. (SEBPO) as executive. His research interests Renewable Energy (Especially Solar Energy), Power Electronics, and Machine Learning.

Md. Rifat Hazari received his B.Sc. Engg. and M.Sc. Engg. Degrees in Electrical and Electronic Engineering from American International University-Bangladesh (AIUB) in August 2013 and December 2014, respectively and Ph.D. Degree in Energy Engineering from Kitami Institute of Technology (KIT), Japan, in March 2019. He served as an Assistant Professor and Lecturer in Electrical and Electronic Engineering department at AIUB and Deputy Director of Dr. Anwarul Abedin Institute of Innovation, AIUB. Currently, he is working as a Senior Assistant Professor and Special Assistant in the Electrical and Electronic Engineering department at AIUB. He received the MINT (Academic Excellence) Award 2017 from KIT for the outstanding research of 2017 academic year, Best Paper Award in the Australasian Universities Power Engineering Conference 2017, Melbourne, Victoria, Australia, Best Presentation Award in the IEEJ Branch Convention 2017, Hakodate, Japan and Best Sustainable Development Goal (SDG) Posterity Award in 3rd International Conference on Robotics, Electrical and Signal Processing Techniques 2023, Dhaka, Bangladesh. He has published more than 75 articles in different journals and international and national level conferences. He has been an invited speaker at many universities and workshops. His research interests are renewable energy systems (especially wind power & photovoltaic power systems), power system stability and control, microgrid and hybrid power systems, HVDC system, analysis and control of rotating electrical machines. Dr. Hazari is a member of IEEE and IEB.

Shameem Ahmad was born in Chittagong, Bangladesh, in 1985. He received his PhD and Master's degree in Electrical Engineering from Universiti Malaya, Malaysia, in 2014 and 2022 respectively. He received his B.E. degree from Visveswaraiah Technological University (VTU), Belgaum, India in Electrical and Electronics Engineering, 2009. He currently working as an Assistant Professor in American International University-Bangladesh (AIUB). His field of interest includes microgrid control & management, inverter control, power system stability and optimization, battery management and charging system for electric vehicle and unmanned unwater vehicle.

Mohammad Abdul Mannan was born in Laxmipur, Bangladesh on January 01, 1975. He received his B. Sc. Eng. Degree from Rajshahi University of Engineering and Technology (RUET former BITR), Bangladesh, in 1998, and Masters of Eng. and Dr. of Eng. degrees from Kitami Institute of Technology, Japan, in 2003 and 2006, respectively, all in electrical engineering. He then joined in the American International University Bangladesh (AIUB) as an Assistant professor in May 2006. He served in AIUB as an Associate Professor from December 2013 to November 2016. Now he is working as a Professor and Associate Dean of the Faculty of Engineering in AIUB. His research interests include electric motor drive, power electronics, power system, wind generation system and control of electric motor, power electronic converters, power system, and wind generation system. Prof. Dr. Mannan is a senior member of the IEEE and fellow of IEB.